CBPF-NF-037/02

Photofissility of Heavy Nuclei at Intermediate Energies

A.Deppman[a], O.A.P.Tavares[b],S.B.Duarte[b], J.D.T. Arruda-Neto[a,c], M. Gonçalves[d], V.P. Likhachev[a], and E.C. de Oliveira[b]

[a)] *Instituto de Física da Universidade de São Paulo*
P.O.Box 66318 - 05315-970 São Paulo, Brazil
[b)] *Centro Brasileiro de Pesquisas Físicas -CBPF/MCT*
22290-180 Rio de Janeiro, Brazil
[c)] *Universidade de Santo Amaro, 04829-300 São Paulo, Brazil.*
[d)] *Instituto de Radioproteção e Dosimetria - IRD/CNEN*
22780-160 Rio de Janeiro, Brazil
and Sociedade Educacional São Paulo Apóstolo- UniverCidade,
22710-260 Rio de Janeiro, Brazil.

October, 2002

Abstract

We use the recently developed MCMC/MCEF (MultiCollisional Monte Carlo plus Monte Carlo for Evaporation-Fission calculations) model to calculate the photofissility and the photofission cross section at intermediate energies for the ^{243}Am and for ^{209}Bi, and compare them to results obtained for other actinides and to available experimental data. As expected, the results for ^{243}Am are close to those for ^{237}Np.The fissility for preactinide nuclei is nearly one order of magnitude lower than that for the actinides. Both fissility and photofission cross section results for ^{209}Bi are in good agreement with the experimental data.

Pacs:25.85.Jg, 25.20.-x, 25.85.-w

Key-words: Photonuclear reactions; Photofission; Photofissility; Intranuclear cascade; Evaporation-fission competition.

The non-saturation of actinide photofissility at intermediate energies was a long-standing puzzle in the field of nuclear fission. It has been recently solved by using two Monte Carlo calculations, namely, the MCEF[1] for the evaporation/fission competition process, and the MCMC[2] for the intranuclear cascade process, which correctly describe the fissility and the photofission cross sections for ^{232}Th, ^{238}U and ^{237}Np target nuclei[3].

The MCMC code describes the intranuclear cascade process using a realistic Monte Carlo calculation where all the hadronic interactions are considered in a time-ordered sequence[2]. In this case, local nuclear-density fluctuations are naturally taken into acount in the calculation. An interesting consequence of this model is that the particle multiplicities are different from those obtained by using the classical Monte Carlo calculations.

The MCEF code performs the calculations for the nuclear evaporation/fission competition following the intranuclear cascade process in the intermediate energy photonuclear reactions. This code also includes, besides fission and neutron-emission channels, also proton and alpha-particle emissions[1].

Due to the previous success of this model, it is interesting to apply it for verifying what happens to the fissility and the photofission cross section at two limits: the heavy mass limit, as for ^{243}Am, and the preactinide region, such as for ^{209}Bi.

For the ^{243}Am the parameter Z^2/A is higher than for the other actinide nuclei, and for this reason its fissility is expected to be higher than that for the ^{237}Np, i.e., it should be very close to 100%.

The preactinide nuclei have fissilities considerably lower than that for the actinide. The main reason for this fact is their higher fission barrier values. It is interesting to verify if the MCMC/MCEF model can correctly describe the fission characteristics for these nuclei as well. Also, being fission a process that occurs at the end of the evaporation process, its probability depends not only on the fission barrier, but also on the separation energies and on the level density parameters for those nuclei which are formed along the evaporation tree, and on the particle multiplicities. These properties are particularly relevant nowadays, in view of the efforts towards a better understanding of the spallation reactions for preactinides and its possible applications, e.g., in the so-called hybrid reactors, or in astrophysical studies.

In this work we use the MCMC/MCEF model to calculate the fissility and the photofis-

sion cross section for ^{237}Am and ^{209}Bi.

Before extending the calculations to preactinide nuclei, a few modifications in the MCEF code are needed. In the calculations for actinide nuclei, the fission barrier is calculated by[4]

$$B_f = C(0.22(A-Z) - 1.40Z + 101.5)MeV\,. \tag{1}$$

In figure 1 we show the fission barrier as a function of the mass number for nuclei at the β-stability line, where

$$Z = \frac{A}{2} - \frac{0.2A^2}{A+200}\,, \tag{2}$$

following two different approaches, and compare them with the expected fission barrier from the liquid drop model with shell corrections (SC)[5]. We observe that for actinides the formula by Guaraldo et al.[4] (see eq. 1) is in better agreement with the SC results than Nix's formula[6], but for less massive nuclei, Nix's approach is better. Also, considering that the residual nucleus formed after the intranuclear cascade process, following the intermediate energy photon absorption by the Bi target, has an average mass number $A \approx 200$, the evaporation/fission competition will take place at nuclei with mass number $150 < A < 200$, where the Nix and the SC curves for the fission barrier have similar shapes and values. Therefore, for the referred nuclei we calculate the fission barrier following Nix's formalism[6], i.e.,

$$B_f = a_s\Big[1 - k\Big(\frac{N-Z}{A}\Big)^2\Big]A^{2/3}F(x)\,, \tag{3}$$

where $a_s = 17.9439$ MeV, $k = 1.7826$, and $N = A - Z$. The function $F(x)$, with

$$x = \frac{Z^2/A}{p(1 - k((N-Z)/A)^2)}\,, \tag{4}$$

and $p = 50.88$ is defined in Ref.[6].

We also modified the calculation of the ratio $r_f = a_f/a_n$, which is now calculated according to Martins et al.[7],

$$r_f = r_0 + a_r(\frac{Z^2}{A} - b_r) \tag{5}$$

where

i) $r_0 = 1$, $a_r = 0.05917$ and $b_r = 34.34$ for $Z^2/A > 34.90$,

ii) $r_0 = 1$, $a_r = 0.08334$ and $b_r = 30.30$ for $31.20 < Z^2/A < 34.00$,

iii) $r_0 = 1.281$, $a_r = -0.01842$ and $b_r = 20.00$ for $24.90 < Z^2/A < 31.20$,

iv) and for $Z^2/A < 24.90$, we adopted $r_0 = 1$, $a_r = 0$ and $b_r = 0$.

The fissility results are shown in figure 2, and compared with those for the nuclei previously analyzed[3]. We observe that the fissility (W) is higher than ~ 0.9 for ^{237}Np in the entire energy range, while saturating, at energies above 400 MeV, around $W = 0.85$ for ^{238}U, and around $W = 0.55$ for ^{232}Th, only above 500 MeV. We notice also that for ^{243}Am the fissility is approximately constant at a value close to 100% in the interval $250 - 400MeV$. In addition, considering the uncertainties in the calculation , we see that the Am-fissilities are equal to those for ^{237}Np in the energy range studied here. This result was already expected, since it is well known that the fissility for heavy nuclei increases with Z^2/A, and, therefore, it could not be smaller for ^{243}Am than it was for ^{237}Np.

For ^{209}Bi the fissility increases between $200MeV$ and $450MeV$, from values around 0.06 to 0.12. In this case we have some experimental data available for comparison at the lower energy range investigated in this work up to about $300MeV$. We note in figure 2 that the calculated fissility for ^{209}Bi is in good agreement with the experimetal results.

At photon energies between 140 MeV and 1000 MeV the photoabsorption cross section is practically proportional to the nuclear mass number A[8–10]. This allows the definition of a universal curve for the bound nucleon photoabsorption cross section, $\sigma_{\gamma,a}(E)$, which is related to the total nuclear photoabsorption cross section, $\sigma_{\gamma,A}(E)$, by

$$\sigma_{\gamma,A}(E) = \sigma_{\gamma,a}(E) A. \tag{6}$$

These quantities are related to the photofission cross section, $\sigma_{\gamma,f}(E)$, by

$$\sigma_{\gamma,f}(E) = A\sigma_{\gamma,a}(E) W. \tag{7}$$

The $\sigma_{\gamma,a}(E)$ curve can be determined from the experimental values for C, Al, Cu, Sn and Pb available in the literature[12]. We evaluated the upper and lower limits for this quantity following the procedure described in [12]. The results and the experimental data we used are shown in figure 3a. We observe that most of the experimental data lies within the chosen limits.

Now, using the MCMC/MCEF model to calculate the nuclear fissility, and the universal curve for $\sigma_{\gamma,a}$, in Fig.3a (we have used the mean value between the upper and lower bounds), we get the expected photofission cross section, $\sigma_{\gamma,f}$. We calculated this quantity for ^{209}Bi and for ^{243}Am, and the results are shown in fig.3b. We observe that for ^{243}Am, where the fissility is approximately constant, the resonant structure around $340MeV$ is quite evident. In the case of ^{209}Bi this structure is not so clear, because the fissility for this nucleus is increasing fast in this energy region.

For ^{209}Bi there are some experimental data available between $200MeV$ and $300MeV$, which are compared with our calculated $\sigma_{\gamma,f}$ in figure 4. We observe a good agreement between our calculation and the experimental data, showing that our model can be extended to the preactinide nuclei if the relevant fission barriers are calculated using Nix's expression (see eq. 3 and Ref.[6]).

Finally, we wish to address the so-called shadowing effect, which has been observed in photo- and electro-nuclear scattering, and it is due to the hadronic structure of the photon. At high energies ($E \gtrsim 1.2GeV$) a photon can dissociate into a bare photon and a quark-antiquark pair, which evolve according to the QCD. This scenario is more easily described in the VDM (Vector Dominance Model), which assumes that the bare photon component practically does not interact with the nucleus, while its hadronic component, usually described as a vector meson (ρ, ω, ϕ), strongly interacts with the nuclear matter (hadron dominance). Thus, the photon-nucleus interaction may be described through the interaction of those mesons with the nucleus. The important parameters are:

i) the photon coherence length, which for real photons is given by

$$l_f = \frac{2\nu}{m_f^2}\,, \tag{8}$$

where m_f is the f-meson mass ($f = \rho, \omega, \phi$), and ν is the photon energy, and

ii) the f-component mean-free-path in the nuclear matter, λ_f. The shadowing effect takes place whenever $l_f \gtrsim \lambda_f$.

The shadowing intensity, and therefore the total photoabsorption cross section, depends thus on the meson-nucleus cross section and on the relative values of l_f and λ_f. This effect can be accounted for in the Monte Carlo calculation for the intranuclear cascade by

including the relevant meson cross sections and the reaction mechanism described above. We are presently working on the inclusion of this mechanism into the MCMC code.

With this extended algorithm, we will be able to calculate photonuclear cross section at energies above $1GeV$, allowing us to study effects such as the meson mass variation in the nuclear matter.

To conclude, in this work we applied the MCMC/MCEF model to the calculation of fissility and photofission cross section at intermediate energies for ^{209}Bi and ^{243}Am.

Our results are in good agreement with the experimental data, providing an explanation for the non-saturation of the fissility for actinide nuclei even at energies as high as 1000 MeV. For the preactinide nucleus ^{209}Bi, we show that our method is still valid, allowing for a correct description of the increasing fissility in the intermediate energy range. In this regard, we would like to mention the very recent paper by Cetina et al[20] reporting, for the first time, accurate results for the ^{nat}Pb photofission cross section from $0.2GeV$ up to $3.8GeV$, measured at the Jefferson Lab. A comparison of these new results with our calculations will soon be performed.

We acknowledge the support from the Brazilian agencies FAPESP and CNPq, and from the CLAF (Latin-American Center for Physics). One of us (A.D.) is thankful for the warm hospitality received during his stay at the CBPF.

---

[1] A. Deppman et al., Comp. Phys. Comm. 145 (2002) 385.

[2] M. Gonçalves et al.; Phys. Lett B406, 1 (1997).

[3] A. Deppman et al., Phys. Rev. Lett. 87 (2001) 182701.

[4] C. Guaraldo et al., Nuovo Cimento. 103A, 607 (1990).

[5] W.D. Myers and W.J. Swiatecki, Nucl. Phys. 81 (1966) 1.

[6] J.R. Nix, Nucl. Phys. A130 (1969) 241.

[7] J.B. Martins et al., Phys. Rev. C44 (1991) 354.

[8] N. Bianchi et al., Phys. Rev. C48, 1785 (1993).

[9] N. Bianchi et al., Phys. Lett. B299, 219 (1993).

[10] Th. Frommhold et al., Phys. Lett. B295, 28 (1992).

[11] M.L. Terranova et al., J. Phys. G: Nucl. Part. Phys. 22 (1996) 1661.

[12] A. Deppman et al., Il Nuovo Cimento 111A, (1998) 1299, and references therein.

[13] V. Bellini et al, Lett. Nuovo Cimento. 36 (1983) 587.

[14] L. G. Moretto et al., Phys. Rev. 179 (1969) 1176.

[15] E.V. Minarik and V.A. Novikov, Sov. Phys. - JETP 5 (1957) 253.

[16] Yu. N. Ranyuk and P. V. Sorokin, Sov. J. Nucl. Phys. 5 (1967) 37.

[17] C. Guaraldo et al., Phys. Rev. C 36 (1987) 1027.

[18] J.A. Jungerman and H.M. Steiner, Phys. Rev. 106 (1957) 585.

[19] J.D.T. Arruda-Neto et al., Phys. Rev. C 34 (1986) 935.

[20] C. Cetina et al., Phys. Rev. C 65 (2002) 044622.

I. FIGURE CAPTIONS

Figure 1: Fission barrier as a function of mass number for nuclei at the β-stability line. The full line represents the calculation according to Nix[6], the dashed line represents the liquid drop model calculation with shell correction[5], and the dash-dotted line represents the calculation according to Guaraldo et al.[4].

Figure 2: Calculated nuclear fissility as a function of incident photon energy for ^{243}Am, ^{237}Np, ^{238}U, ^{232}Th and ^{209}Bi. A few experimental data for bismut[11] are also shown.

Figure 3: **(a)** Universal bound nucleon photoabsorption cross section as a function of incident photon energy (see text). The full lines represent the upper and lower limits for the bound nucleon photoabsorption cross section; **(b)** Nuclear photofission cross section calculated according to the model described in this work, for ^{209}Bi and ^{243}Am target nuclei.

Figure 4: Photofission cross section for ^{209}Bi deduced in this work in the range $200 - 500MeV$. We compare our results (full line) with availabe data from literature. The experimental data are as follows: open squares [13], open circles [14], open triangles [15], full squares [11], full circles [16], full triangles [17], open rhombi [18], and dashed line [19].

Figure 1

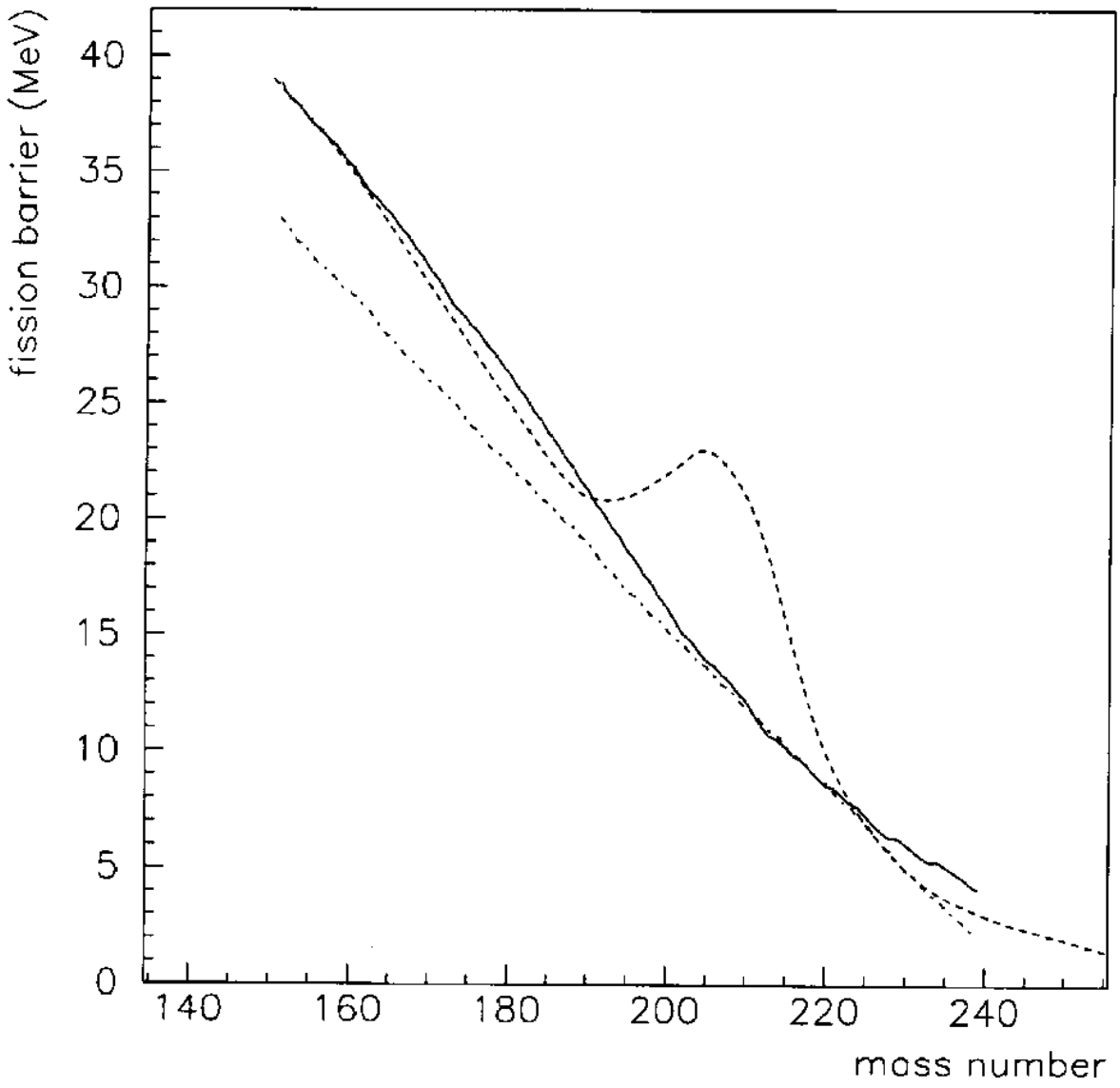
fission barrier (MeV)
40
35
30
25
20
15
10
5
0
140
160
180
200
220
240
mass number

Figure 2

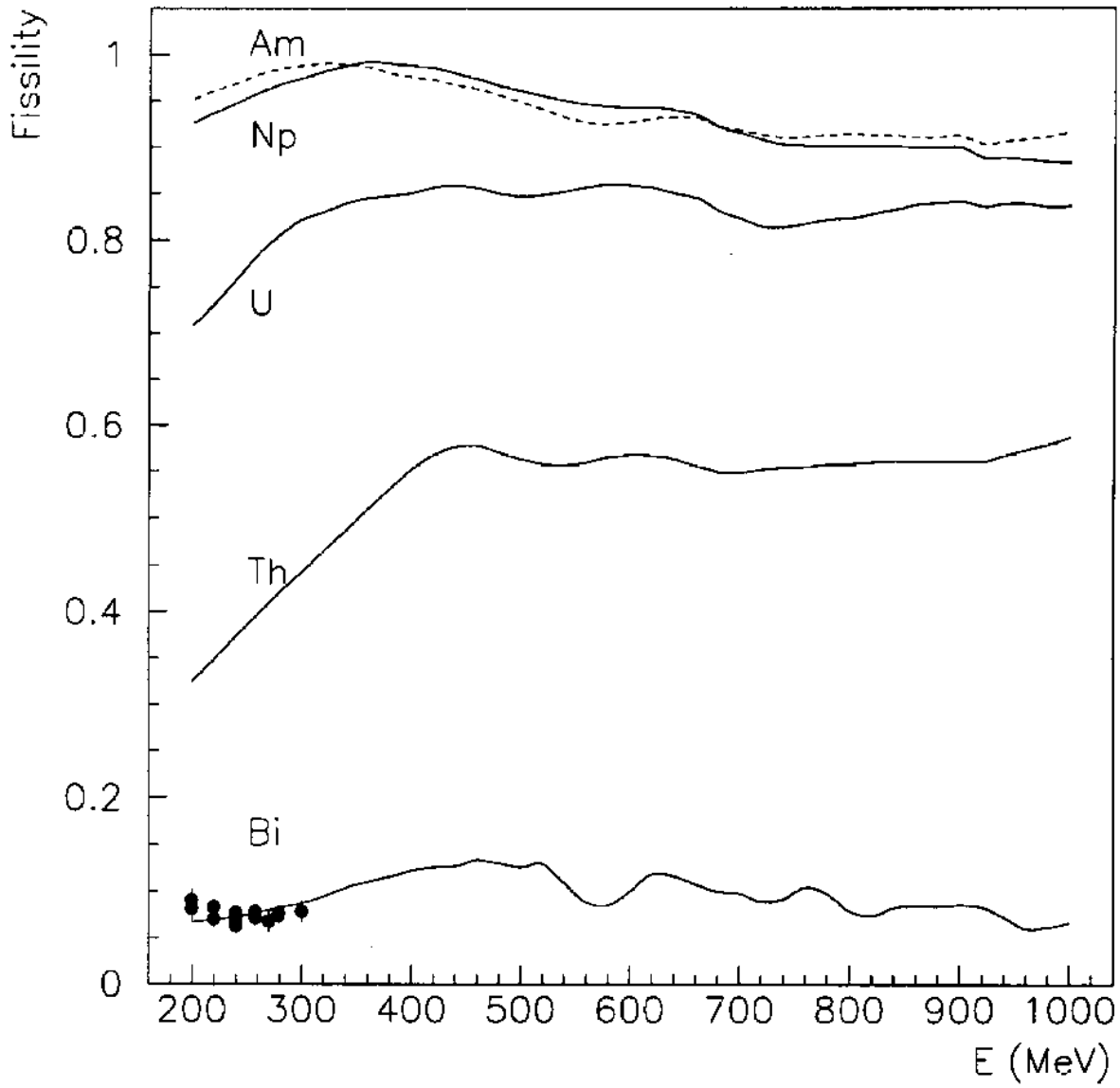
Fissility
1
0.8
0.6
0.4
0.2
0
Am
Np
U
Th
Bi
200
300
400
500
600
700
800
900
1000
E (MeV)

Figure 3

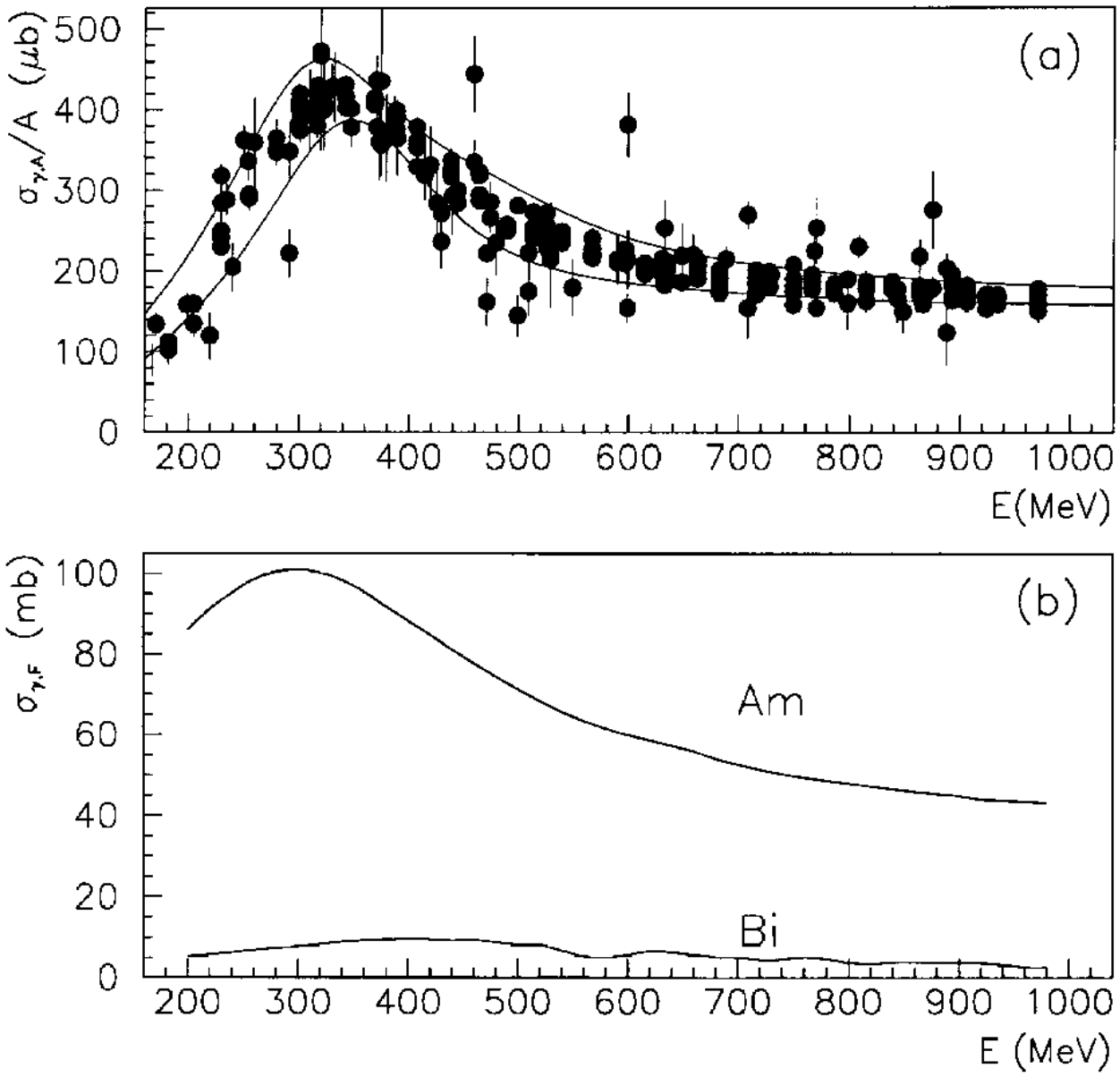
(a)
$\sigma_{\gamma,A}/A$ (μb)
0
100
200
300
400
500
200
300
400
500
600
700
800
900
1000
E(MeV)
(b)
$\sigma_{\gamma,F}$ (mb)
0
20
40
60
80
100
Am
Bi
200
300
400
500
600
700
800
900
1000
E (MeV)

Figure 4